Statistical analysis for fatigue life evaluation of woven E-glass/epoxy composite laminates containing off-centre interacting circular holes

**Bhaskara Rao Pathakokila[1] · Ramji Koona[2] ·
Rama Krishna Avasarala[2] · Satya Devi Ambadipudi[3] ·
V Manoj Kumar Uppuluri[4]**

Abstract Fatigue behaviour of woven E-glass/epoxy composite laminates containing off-centre interacting circular holes was determined under sinusoidal loading in tension–tension at 0.1 stress ratio. Laminate samples with central hole were also investigated. Tensile and fatigue tests were conducted on specimens in load control mode. For the unnotched, central holed and off-centre interacting holed laminates, fatigue life was evaluated using a two-parameter Weibull distribution function at different probabilities and confidence levels. Results indicated that the number of samples taken at each stress level of fatigue experiments is adequate for the S–N curve generation at 90% confidence level and 90% Weibull probability. From the traditional and mean S–N curves, the effect of scatter on fatigue strengths of the specimens was investigated. Life distribution graphs were constructed to determine the fatigue life at any survival per cent. Damage forms and the associated causes were also explained.

Keywords Off centre · Fatigue life · Weibull distribution · Statistical analysis · Scatter · Reliability

1 Introduction

Composites are an alternative for weight critical applications instead of metals due to their high specific stiffness and strength. Aircraft, spacecraft, automobile and marine structures

✉ Bhaskara Rao Pathakokila
  bhaskarengg@yahoo.com

[1] Department of Mechanical Engineering, Vignan's Lara Institute of Technology & Science, Vadlamudi 522 213, Andhra Pradesh, India

[2] Department of Mechanical Engineering, Andhra University College of Engineering, Visakhapatnam 530 003, Andhra Pradesh, India

[3] Department of Aerospace Engineering, Gandhi Institute of Technology and Management, Hyderabad 502 329, Telangana, India

[4] Department of Mathematics, Vignan's Foundation for Science, Technology and Research, Vadlamudi 522 213, Andhra Pradesh, India

are some of the engineering applications. In these applications, variable loading under repeated cycles is very common, which causes eventual fatigue in composite structures. A composite material is inhomogeneous and anisotropic, therefore its response is completely different from that of metal under fatigue loading (Degrieck and Paepegem 2001). Fatigue in metals is a localised and progressive process which occurs in a single mode of failure by the initiation of a crack, which propagates to critical size and then a final fracture occurs (Wicaksono and Chai 2012). Composites build up multiple damage modes such as fibre breakage, matrix cracking, delamination and debonding of fibre from matrix. These damage modes develop simultaneously and follow complex growth patterns independently or with mutual interaction (Satapathy et al. 2013). Hence, the combined contribution of damage modes leads to the complexity of understanding the fatigue behaviour of fibre-reinforced composites. It is therefore an important issue to be considered by the designer for structural applications. In the context of aforesaid applications for many decades' fatigue experiments have been conducted for a wide range of composite systems to determine fatigue life. However, material's inhomogeneity and variability in manufacturing processes are important factors resulting in fatigue scatter, but the stress distribution due to holes is another one that also contributes to a large scatter in fatigue experiments. This scattered nature occurs even when the specimens are collected from same lot and tested in same conditions. Although new test methodologies (Maillet et al. 2013) were developed to run fatigue tests at resonant frequencies in high cycle and gigacycle regimes, they are mostly used for metallic materials to observe the behaviour of gigacycle fatigue (Marines et al. 2003; Sohar et al. 2008). For this reason, one cannot avoid conventional fatigue testing systems for the investigation of high cycle fatigue properties of composites. Whether the test methodologies are new or conventional, fatigue tests are normally considered time consuming and costly. Therefore, one cannot test too many samples for determining fatigue life. On the other hand, as it is very difficult to predict fatigue life from a limited number of specimens due to the scatter in the experimental data; statistical evaluations are essential because of different distributions of test results in FRP samples.

Typical investigations reported in the literature on scatter and fatigue life distributions of composites are presented here. Frost et al. (1974) described that fatigue experiments with sample size of two to four specimens upon careful selection produce results with minimum error. According to Parida et al. (1990), error occurs in results regardless of the sample size and mainly depends on the confidence level, probability of survival, and stress level. For the fatigue life of FRP materials, studies (Yang and Jones 1978; Yang et al. 1980; Shimokawa and Hamaguchi 1981) conducted with small sample sizes produced large scatter, and this data did not fit to any of the distributions. However, fatigue lives of composite samples tested with various sample sizes under same conditions would follow normal distribution with constant standard deviation (Shimokava and Hamaguchi 1983). A two-parameter lognormal (Ratnaparkhi and Park 1986; Hwang and Han 1987) and Weibull (Hwang and Han 1987; Sakin and Irfan 2008) distribution models were employed for determining scatter in fatigue data and life distributions of glass fibre-reinforced epoxy composites. Recently, Liu et al. (2017) and Marwa et al. (2017) used Weibull distribution function for the assessment of failure probabilities of polymeric composites. Gope (1999) designed a method to determine sample size for estimating fatigue life at desired probability of survival, confidence level and maximum acceptable error for the data that follows Weibull distribution. Several graphical methods were also suggested by the researchers (Parida et al. 1990; Gao 1984; Nakazawa and Kodama 1987; Gope 1994) to evaluate the fatigue life from a limited amount of data. However, Weibull distribution gave more reliable values than other distribution models hence it is useful in the fatigue analysis of composite structures (Hwang and Han 1987; Sakin and Irfan 2008; Khashaba 2003; Liu et al. 2017; Marwa et al. 2017).

In a large transport aircraft, millions of holes (Khashaba et al. 2010) are drilled to receive bolts and rivets. These holes in composites produce serious problems of stress concentrations due to geometric discontinuity and anisotropic behaviour of material. This is a situation of the interaction of stress concentrations in the material occurring due to the proximity of circular holes under certain loading conditions. The overall strength of a composite depends on the size of the hole, distance between holes, number of holes, their locations, effect of layup and ellipticity of holes (Xu et al. 2000). Ghezzo et al. (2008) studied the overall stress concentration produced in axially loaded composite laminates with two holes with respect to change in centre distance, size and position of the holes. The hole patterns and densities also effect the failure modes in addition to strength of the composite (Kazemahvazi et al. 2010) due to change in hole interaction. The stress concentration factor around the interacting circular holes can be reduced by introducing defence holes (Meguid and Gong 1993) to increase the fatigue life. Wei-xun and Jian-guo (1988) discussed stress concentration in a laminate weakened by multiple holes of close proximity in series. They noticed higher stress concentration at the inner holes than the outer holes when the direction of loading was perpendicular to the line of hole centres. Soutis et al. (1991) studied the compression fatigue behaviour of $[(\pm45/0_2)_3]_S$ carbon/epoxy laminates containing two transverse closely spaced holes at equidistant from loading axis and observed the interaction of damage between two holes. Delamination and matrix splitting were observed as the significant damage modes. The matrix splitting at the outer edges of holes served to reduce stress concentration factor. Ferreira et al. (1997) studied the effect of stress concentration induced by the off-centre transverse holes on the fatigue strength of a glass-fibre-reinforced composite and concluded that both the size and position of off-centre hole alter the damage modes.

In continuation to the literature available on few studies of fatigue performance of composite laminates with off-centre holes, the present paper focuses on the investigation of the fatigue life of plain weave E-glass/epoxy composite laminate containing a central hole and two interacting circular holes drilled off the loading axis at different angular positions. Consequently, statistical evaluation was done using a two-parameter Weibull distribution to determine the amount of scatter and error involved in fatigue experiments conducted in tension–tension for the predetermined sample size.

2 Experimental

The composite used in this study consisted of E-glass fabric reinforced with epoxy (Araldite LY556) with a volume fraction of 0.65. This fibre volume fraction was calculated directly on the composite material. A plain woven roving glass cloth of grade 7 mil was used as the reinforcing material. Two hardeners of grades K-10 and K-86 were used with the resin for reinforcement. For every 100 parts of resin, 35 parts of K10 and 1 part of K86 were added. Raw material was supplied by M/S Atul & Huntsman Ltd. Laminate thickness was 2.1 mm. Each laminate consisted of 12 layers of glass cloth (0.17 mm). The laminates were manufactured and supplied by M/S Texplas India (Pvt) Ltd., Hardwar, Uttarakhand, India in the sizes of 800 mm × 800 mm × 2.1 mm.

Araldite (standard epoxy adhesive) manufactured by M/S Huntsman Advanced Materials (India) Pvt Ltd was used with equal parts of epoxy and hardener for adhering the ends of the specimens to aluminium tabs on both sides to prevent slipping and crushing of their ends in the grips during testing. The contact surfaces of the aluminium tabs and specimen ends were roughened with electro-coated abrasive paper of grade 50 before bonding. The bonded

Fig. 1 Test samples:
(**a**) unnotched specimen and
(**b**) specimen with interacting
circular holes
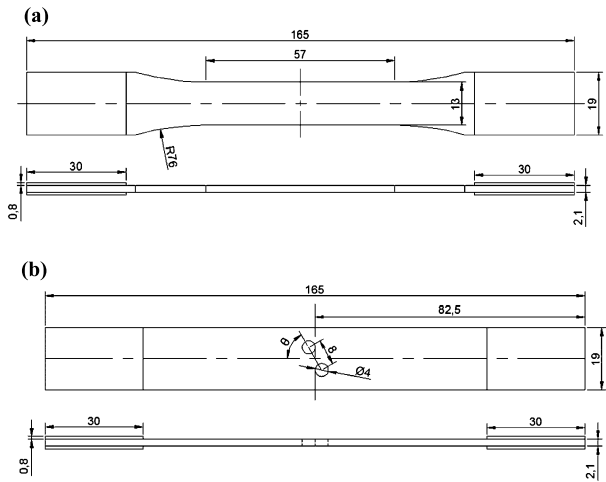
assembly of specimen with end tabs was placed under pressure for 24 hours in a mechanical vice and tested then.

Figure 1(a) shows the configuration of an unnotched specimen which conforms to ASTM D 638-08, type 1. A specimen containing two circular holes drilled off the loading axis on both sides and their centre line at a certain angle (θ) is shown in Fig. 1(b). From this configuration, two different test samples with centre line of holes at 30° and 60° off the loading axis were derived. The holes were closely spaced with the centre distance being twice the diameter. Therefore, they are named interacting circular holes due to their mutual influence on the specimen performance and with this convention, discussions are done in this paper. The holes were drilled with a diamond core drill. Static tests were conducted on a 20 kN tensometer at a cross-head speed of 0.2 mm/min. Six specimens were tested for determining ultimate tensile strength (σ_u), and their average was considered. Tensile strengths of the specimens were determined on the basis of net cross-sectional area (A). For unnotched specimens, the cross-sectional area was taken in the portion of gage length of 57 mm. The cross-sectional area for central holed laminates equals to $(b - d)t$. The parameters b, d and t represent width, hole diameter and thickness of the specimen, respectively. For both types of off-centre holed samples, also the same cross-sectional area $(b - d)t$ was considered in the determination of ultimate tensile strength because if one assumes a transverse section on the diameter of one drilled hole, the section does not contain the other hole. The ultimate tensile strength of specimens was determined using Eq. (1) given below:

$$\sigma_u = \frac{P}{(b - d)t}. \tag{1}$$

In Eq. (1), P is the maximum applied load. The tensile strengths of the specimens are presented in Table 1. The failure of the composite under tensile loads is fibre-dominated and for compressive loads the role of matrix, fibre misalignment and material defects is more pronounced. Hence, one can design a testing program based on the loads examined in the material application (Vassilopoulos 2010). In fact, to study the performance of the composite under ideal tensile cyclic load, the specimen should be fatigued between zero and some positive load. This may produce any overshoot into compression. To overcome its occurrence, a positive minimum load at the bottom of the cycle is used while conducting fatigue experiments (Gathercole et al. 1994). This consideration results in a positive stress ratio (R) for

Table 1 Mechanical properties from tensile test

Specimen type	σ_u (MPa)	Standard deviation
Unnotched	316.56	4.21
Central holed	201.37	3.76
30° off-centre	172.57	5.92
60° off-centre	144.73	6.04

tensile–tensile fatigue tests. For the design of components, a stress ratio of 0.1 is often used in structural applications. Therefore, at this stress ratio ($R = 0.1$), fatigue tests were run with sinusoidal loading on the specimens at consecutive stress levels from 0.8 to threshold with 0.1 decrement. The ratio of maximum cyclic stress ($\sigma_{\max}$) to the ultimate tensile strength (σ_u) of the virgin specimen is considered as the stress level. Three different frequencies of 3 Hz (at stress levels 0.8 and 0.7), 4 Hz (at stress levels 0.6 and 0.5) and 5 Hz (at stress level less than and 0.4) were used. The fatigue tests were conducted in load control mode on servo-hydraulic 10 kN single axis fatigue testing machine. A load cell of 20 kN capacity was used to monitor the fatigue load. At each stress level, five specimens were fatigued and no failure occurred in the grips. The fatigue tests were terminated when the number of cycles of load application on the specimen exceeded one million and no damage was seen on the specimens prior to reaching one million cycles. Moreover, no failure of the specimen occurred at one million cycles. The failure could mean here complete physical separation of the specimen material in both static and fatigue tests.

3 Weibull analysis

For the two-parameter Weibull distribution (Sakin and Irfan 2008; Gope 1999; Khashaba 2003; Marwa et al. 2017; Liu et al. 2017), the cumulative distribution function is given as

$$F_{N_f}(N_f) = 1 - \exp\left\{-\left(\frac{N_f}{\theta}\right)^{\beta}\right\}, \tag{2}$$

$$F_s(N_f) = 1 - F_{N_f}(N_f). \tag{3}$$

Applying logarithm on both sides of Eq. (3) results in

$$\ln\left[\ln\left(\frac{1}{F_s(N_f)}\right)\right] = \beta \ln(N_f) - \beta \ln(\theta). \tag{4}$$

From Eq. (4), it has been observed that the relationship between $\ln[\ln(\frac{1}{F_s(N_f)})]$ and $\ln(N_f)$ is linear, representing a straight line. The slope of this line is Weibull slope or shape parameter (β); θ is the characteristic fatigue life, or scale parameter.

If $x = \ln(N_f)$ follows an extreme value distribution function (Gope 1999), assuming $\delta = \frac{1}{\beta}$ and $\xi = \ln(\theta)$, Eq. (2) may be written as

$$\exp\left\{\frac{x - \xi}{\delta}\right\} = \left(\frac{N_f}{\theta}\right)^{\beta},$$

$$F_x\left[\ln(N_f)\right] = 1 - \exp\left\{-\exp\left(\frac{x - \xi}{\delta}\right)\right\}. \tag{5}$$

At α percent of probability and γ percent of confidence level,

$$\text{safe fatigue life } (\mu_x) = \overline{x} + (d + \lambda)\overline{\delta}. \tag{6}$$

In Eq. (6),

$$\overline{x} = \overline{\overline{\xi}} + \lambda\overline{\delta} \quad \text{and} \quad \lambda = \ln\left[-\ln(1-\alpha)\right].$$

The coefficient of variation of Weibull distribution is

$$(\phi_w) = \frac{\overline{\delta}}{\mu_x + (d+\lambda)\overline{\delta}}, \tag{7}$$

in which $d = \{\frac{-a_{12}u^2 - n\lambda + u\varepsilon}{n - a_{22}u^2}\}$ and $\varepsilon = [(-a_{12}^2 - a_{11}a_{12})u^2 + na_{11} + 2na_{12}\lambda + na_{22}\lambda^2]^{0.5}$.

Assuming the sample life to be population life,

$$\text{Percentage of error } (R_w) = \frac{E(\mu_x) - \mu_x}{\mu_x} \times 100, \tag{8}$$

$$\text{Error factor } (K_{\omega,\alpha,\gamma}) = \frac{R_w}{\phi_w}. \tag{9}$$

The values of a_{11}, a_{22}, a_{12} and the error factors reported by Gope (1999) were taken for the analysis.

In the above equations,

$F_{N_f}(N_f)$ is the probability of failure;
$F_s(N_f)$ is the probability of survival, or reliability;
x is a variable which represents the number of cycles to failure (N_f);
$\overline{x}, \overline{\xi}, \overline{\delta}$ denote parameters determined from sample data;
u is a normal deviate corresponding to probability of failure (α);
a_{ij} are the coefficients for the Asymptotic Variances and Covariance of $\frac{\overline{\delta}}{\delta}$ and $\frac{\overline{\overline{\xi}}}{\xi}$;
μ_x is the expected population;
$E(\mu_x)$ is the sample life.

The Weibull statistical properties (Sakin and Irfan 2008; Khashaba 2003; Marwa et al. 2017) such as mean life, also called mean number of cycles to failure (N_o), standard deviation (SD) and coefficient of variation (CV) of the two-parameter Weibull distribution can be calculated from the following expressions:

$$\text{Mean number of cycles to failure } N_o = \overline{\theta} \cdot \Gamma\left(1 + \frac{1}{\beta}\right); \tag{10}$$

$$\text{Standard deviation } (SD) = \overline{\theta} \cdot \left[\Gamma\left(1 + \frac{2}{\beta}\right) - \Gamma^2\left(1 + \frac{1}{\beta}\right)\right]^{\frac{1}{2}}; \tag{11}$$

$$\text{Coefficient of variation } (CV) = \frac{SD}{N_o}. \tag{12}$$

4 Weibull distribution to fatigue life data

The Weibull slope ($\overline{\beta}$) and characteristic fatigue life ($\overline{\theta}$) are the distributional parameters determined from sample data (Gope 1999). In order to determine these parameters, $\ln[\ln(\frac{1}{F_s(N_f)})]$ was plotted against $\ln(N_f)$ for each N_f. This was implemented using

Table 2 Distributional parameters for fatigue lives of unnotched specimens at 0.5 stress level

σ_{max} (MPa)	N_f	Distributional parameters				
		$\overline{x}$	$\overline{\beta}$	$\overline{\delta}$	$\overline{\theta}$	$\overline{\xi}$
158.28	14682	9.48	6.62	0.15	14131.05	9.55
	13542					
	10367					
	15399					
	12253					

Table 3 Error for fatigue life prediction of unnotched samples at 0.5 stress level

Confidence level	90%		95%	
Weibull probability	90%	95%	90%	95%
σ_{max} (MPa)	Error			
158.28	0.028	0.039	0.028	0.048

Table 4 Weibull statistical properties for unnotched specimens at 0.5 stress level

σ_{max} (MPa)	N_o	SD	CV
158.28	13184.83	2320.67	0.17

Weibull++. It is a software for Weibull analysis; its version 9 was provided by Relia Soft Corporation. Other distributional parameters $\overline{x}, \overline{\xi}$ and $\overline{\delta}$ for the fatigue life data at various maximum cyclic stresses and the corresponding parameters $\lambda, \varepsilon, d, \mu_x$ and ϕ_w at 90% and 95% Weibull probabilities were determined using Eqs. (5)–(7). The normal deviate (u) at each of these probabilities of failure was taken from the normal distribution tables. The values of error factor ($K_{\omega,\alpha,\gamma}$) at α% of probability and γ% of confidence level were taken from the tables reported in Gope (1999). The percentage of error (R_w) has been determined using Eq. (8).

5 Results and discussion

5.1 S–N curves

The fatigue data of unnotched samples obtained at 50% of ultimate tensile strength were used for typical calculations of distributional parameters, error in fatigue life and Weibull statistical properties presented in Tables 2, 3, 4. The S–N curves drawn on semi-log paper with mean fatigue lives (Sakin and Irfan 2008; Khashaba 2003) are shown in Fig. 2(a). From these curves, fatigue strengths of 96.32, 48.17, 59.09 and 46.30 MPa have been determined respectively at one million cycles for unnotched, central holed, 30° and 60° off-centre interacting notched specimens. But the traditional stress-life curves drawn in Fig. 2(b) gave the corresponding fatigue strengths of 95.04, 53.35, 58.64 and 45.56 MPa for the same samples. The results from mean and traditional S–N curves agreed for unnotched, 30° and 60° off-centre interacting notched specimens. But one can notice a little variation in fatigue strengths of the central holed samples from the same mean and traditional S–N curves, which can be attributed to the wide scatter in fatigue lives which occurred between 10^4–10^5 cycles due

Fig. 2 Fatigue test data plotted for (**a**) mean S–N curves and (**b**) traditional S–N curves
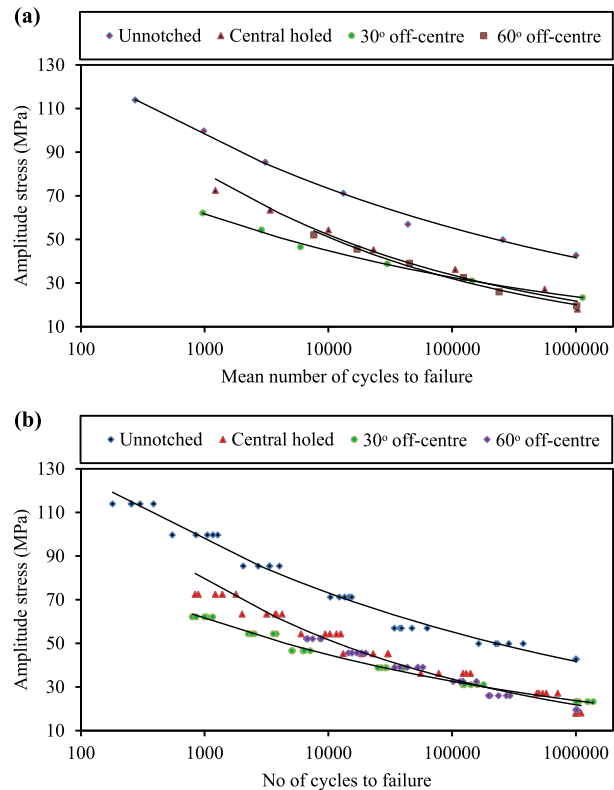
to long delamination induced at lower stress levels (Marwa et al. 2017). The central holed samples have lower fatigue strength than the unnotched due to stress concentration induced by the hole.

The existence of two or more holes in close proximity on a structure such as aero structure produces higher stress concentrations depending upon loading conditions. These stress concentrations may interact and influence the overall stress concentration produced (Graham et al. 2005; Ghezzo et al. 2008; Kazemahvazi et al. 2010). As a result, the interacting stress concentrations can decrease fatigue life of the structure compared to the situation involving a single hole under same loading conditions. This could be the reason for off-centre interacting holed samples having fatigue strengths lower than central holed samples. The significant rise in stresses caused by two or more holes placed in close proximity is useful to the designer for predicting the fatigue life of the structure effectively. The misallocated holes, extra holes and extra notches produced during structural repair are some of the sources of interacting stress concentrations. Furthermore, one can notice the stress concentration factor for orthotropic laminates loaded at an angle from their principal directions varying between 0 to 8 times the global stress applied (Jones 1998). But, the off-axis [±45] orientation reduces the global stress concentration to approximately 1.7 times the global stress (Mohamed et al. 2016). Two different significant damage modes, delamination (led by matrix cracks) in the transverse and matrix splitting in the loading directions, were noticed on the off-centre holed laminates. During cyclic loading, no matrix cracks or delamination appeared at the free edges of central and off-centre holed test coupons.
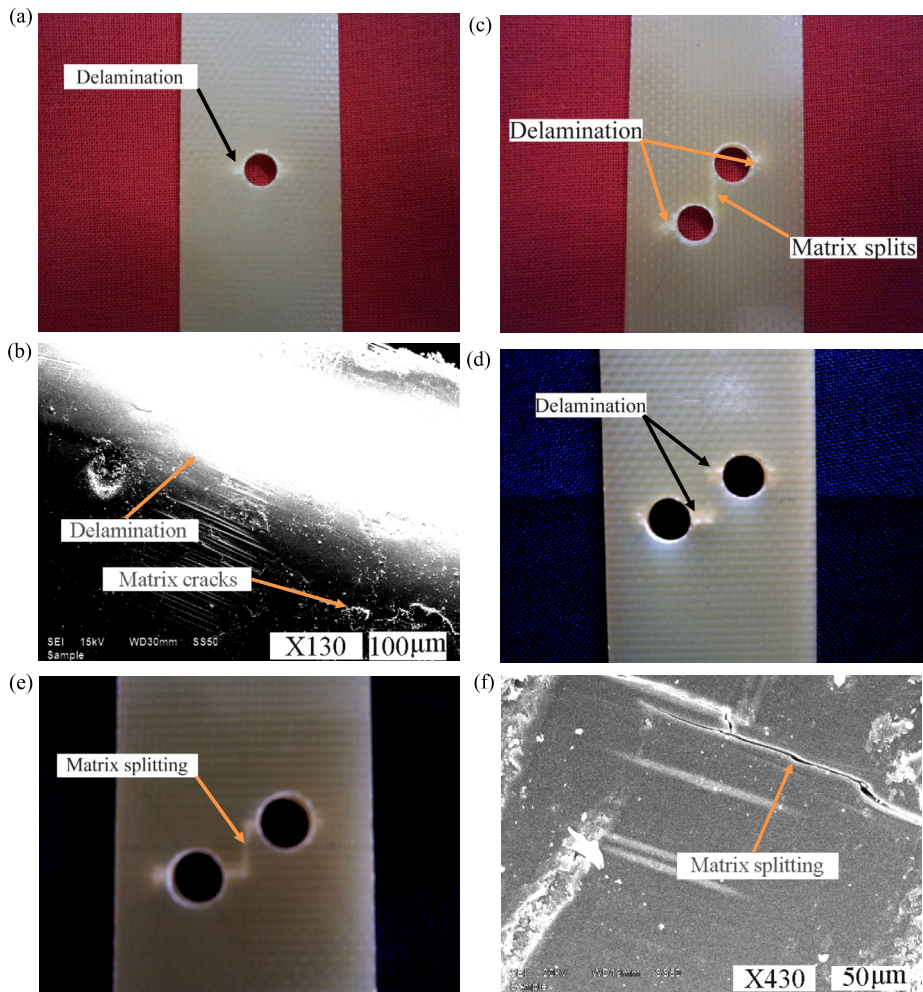
Fig. 3 Damage on fatigued specimens: (**a**) Delamination on central holed; (**b**) SEM image of central holed representing delamination; (**c**) Delamination and matrix splits on 30° off-centre holes; (**d**) Delamination on 60° off-centre holes; (**e**) Matrix splitting on 60° off-centre holes; and (**f**) SEM image of a 60° off-centre holes showing matrix split

On central holed specimens, the mode of damage was delamination in form, which occurred in the transverse direction to the load axis. The damage began from both sides of the hole due to higher stress concentration at the edges and grew toward the free edges of the specimen as in Fig. 3(a). The rate of damage was same on both sides of the hole with respect to load cycles due to uniform distribution of stress, and failure occurred in the plane at 90° to the loading direction. Long delamination with many matrix cracks was induced at lower stress levels as evident by an SEM image in Fig. 3(b) of a central holed specimen sectioned along the load axis after fatiguing for certain number of load cycles at 30% σ_u. However, the damage evolution (i.e. delamination) on specimens containing 30° off-centre holes occurred from the hole edge initially on the thinner side as seen in Fig. 3(c) due to higher stress concentration. This was due to less net cross-sectional area of specimen on the

thinner side of the hole, which indicates that the force lines could pass primarily through the sections of thinner sides at the holes. When stress concentration was reduced to more uniform net section stress, a transfer of tensile load from end to end of the specimen began through the section of bridge between both holes. Hence, the damage mode was changed to loading direction inducing splits tangential to the hole edges on wider sides. These splits began growing in length from the root of one hole to the other with respect to the number of load cycles as in Fig. 3(c). Here, root is defined as a point where the diameter perpendicular to the load axis intersects the wall of the hole. When these splits grew to the critical size, the damage on the thinner side of the hole propagated at a faster rate under repeated cycles and the final failure occurred.

Coming to specimens containing 60° off-centre holes, delamination occurred on both sides of the hole and propagated from the walls to the free edges as seen in Fig. 3(d) due to the load transferred at first across the sections of both wider and thinner sides. On the wider side, damage growth was relatively higher compared to that of the thinner side with respect to load cycles. It signifies that the stress concentration was relatively higher at the root of the hole on the broader side. The mode was subsequently changed to loading direction as the force lines could pass through the longitudinal section between the outer boundaries of delamination on wider sides of the drilled holes and appeared in the form of matrix splits and grew in length towards the holes. These matrix splits served as a boundary to stop the evolution of delamination in the transverse direction on the wider side as viewed in Fig. 3(e). As noted in the case of a test coupon with 30° off-centre holes, the splits on 60° off-centre holed specimens grew to the critical size as viewed in Fig. 3(f) till the stress concentration was reduced. The damage evolution further began to occur on the thinner side with stress cycles, and fracture took place. For the specimens with 30° and 60° off-centre holes, failure occurred on planes at 90° on the thinner sides and 0° to the loading direction.

5.2 Error in the fatigue life

The error percentages of fatigue lives were plotted with respect to maximum cyclic stress in Fig. 4 for unnotched, central and off-centre holed specimens. It can be noticed that the percentage of error increases with an increase in percentage of confidence level and probability. However, the error at 90% and 95% confidence levels for the two different probabilities considered is approximately same. The error at 90% confidence level and 90% Weibull probability is within the minimum acceptable error for all specimens. Moreover, for 30° and 60° off-centre interacting holed specimens, the error at (i) 90% confidence level at 90% and 95% Weibull probabilities and (ii) 95% confidence level and 90% Weibull probability is within the acceptable limit. A large scatter in lifetime for a higher amplitude of fatigue test results in more error (Sakin and Irfan 2008; Khashaba 2003). This was noticed particularly at 95% confidence level with 90% and 95% Weibull probabilities.

5.3 Scatter in fatigue life

The specimens or components identical in shape when tested under same stress levels normally fail at different cycles with large variations. The reasons for scatter in lifetime could be environment, geometry of part, stress level, frequency and void content (Gope 2012). The change in failure mode at a certain stress level and variation in static strength of the material are also the sources of scatter in the fatigue data according to Barnard et al. (1985). The degree of scatter depends on the failure mode. In order to describe the scatter of fatigue
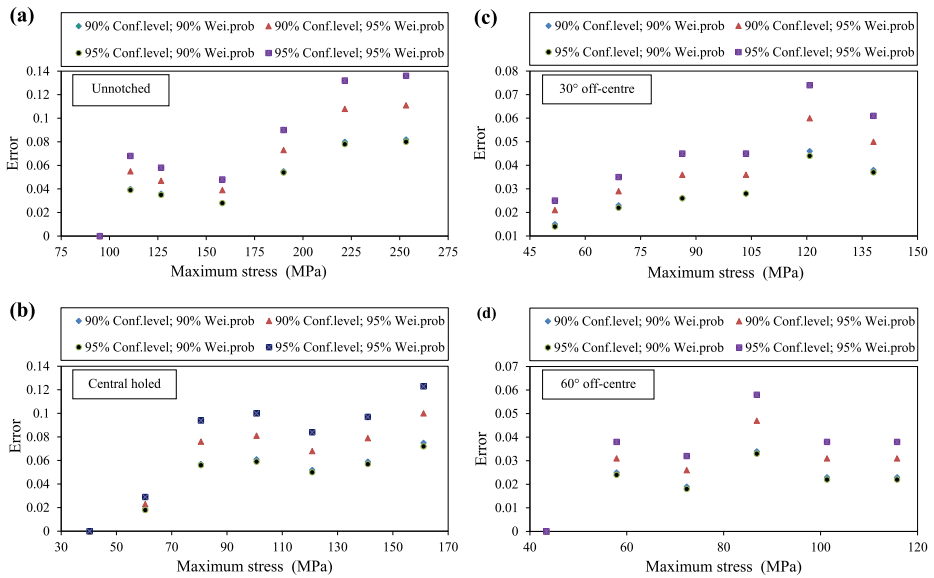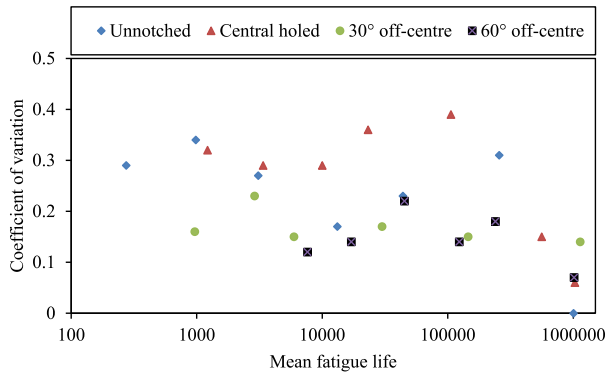
Fig. 4 Variation of error with maximum stress: (**a**) unnotched, (**b**) central holed, (**c**) 30° off-centre, and (**d**) 60° off-centre interacting notched samples

Fig. 5 Influence of mean fatigue life on the coefficient of variation

data, coefficients of variation determined using Eq. (12) were plotted against mean fatigue life in Fig. 5 for all test samples. The values of coefficients of variation range from 0.06 to 0.39. According to these results, for unnotched specimens the scatter was widest between 10^2–10^4 cycles for stress levels above 0.6 due to fibre debonding, fibre misalignment and stress concentration near the broken fibres. The local fibre-matrix debonds could be the reason for the widest scatter from 10^5 to 10^6 cycles at stress levels lower than 0.4. For central holed samples, at stress level 0.8, the failure was mainly due to short delamination followed by breakage of fibres and the fatigue life had high scatter at 10^3 cycles. For the same central holed samples, the failure was caused by long delamination at stress levels 0.4 and 0.5. The scatter in fatigue life at these stress levels was higher between 10^4–10^5 cycles. Further, the failure mode at 0.7 stress level was short delamination on the thinner side of the hole with a scatter in fatigue life between 10^3–10^4 for 30° off-centre holed specimens. A little scatter in fatigue life was noticed for 60° off-centre interacting notched laminates between 10^4–10^5
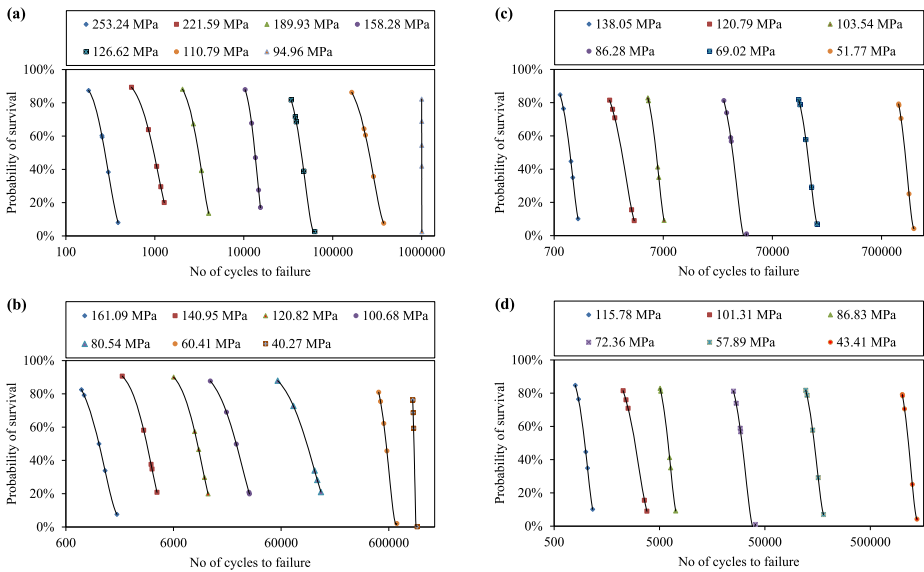
Fig. 6 Diagrams of fatigue life distribution at various stress levels for (**a**) unnotched, (**b**) central holed, (**c**) 30° off-centre and (**d**) 60° off-centre interacting holed samples

and 10^5–10^6 cycles due to change in damage mode from delamination to longitudinal matrix splits. Finally, it is clear that the scatter in fatigue lives between 10^2 and 10^6 cycles is larger comparatively for unnotched and central holed specimens than 30° and 60° off-centre interacting holed specimens. Nevertheless, the scatter of fatigue lives at each stress level of the experiments is very small in comparison with the literature reported (Sakin and Irfan 2008; Khashaba 2003).

5.4 Reliability analysis of fatigue test data

Reliability is defined as the probability of survival of a component to perform the functions (for which it is designed) under a given set of operating conditions in a specific time period (Sakin and Irfan 2008; Khashaba 2003). In the present article, reliability of unnotched samples and coupons with central and off-centre holes has been determined using a two-parameter Weibull distribution function. Equation (3) was used to determine reliability values at each stress level and plotted on semi-log paper against the number of cycles to failure as shown in Fig. 6. The curves of fatigue life distribution drawn in Figs. 6(a)–(d) are of great importance to the designer, and from these curves the fatigue life at any survival percentage can be easily determined. If one assumes a line, for example, horizontally at 50% survival life, the intersecting points on the distribution curves represent 50% survival life at various stress levels.

6 Conclusions

A two-parameter Weibull distribution model has been employed for the fatigue life evaluation of GFRP samples with central and off-centre holes. As fatigue experiments were

conducted at each stress level taking five specimens, error percentages have been calculated at various probabilities and confidence levels. Weibull statistical properties were determined and reliability curves were also generated.

- The error at all stress levels for the number of specimens employed is less than the acceptable limit for 90% confidence level and 90% Weibull probability. Hence, the sample size is adequate to generate traditional S–N curves.
- Weibull statistical properties were determined to generate mean S–N curves. The results of traditional and mean S–N curves have good agreement.
- The maximum coefficient of variation of fatigue life is less than that reported for GFRP composites (Khashaba 2003). Hence, the observed scatter in fatigue life is very small.
- Diagrams of fatigue life distribution are constructed to determine fatigue life at any survival percentage.

Publisher's Note   Springer Nature remains neutral with regard to jurisdictional claims in published maps and institutional affiliations.

References

Barnard, P.M., Butler, R.J., Curtis, P.T.: Fatigue scatter of UD glass epoxy, a fact or fiction? In: Proc. 3rd Conference on Composite Structures, pp. 69–82 (1985)

Degrieck, J., Paepegem, W.V.: Fatigue damage modelling of fibre-reinforced composite materials: review. Appl. Mech. Rev. **54**(4), 279–300 (2001)

Ferreira, J.A.M., Costa, J.D.M., Richardson, M.O.W.: Effect of notch and test conditions on the fatigue of a glass fibre reinforced polypropylene composite. Compos. Sci. Technol. **57**, 1243–1248 (1997)

Frost, N.E., Marsh, K.J., Pook, L.P.: Metal Fatigue. Clarendon Press, Oxford (1974)

Gao, Z.: The confidence level and determination of the minimum of specimens in fatigue testing. In: Proceedings of 2nd International Conference on Fatigue and Fatigue Threshold, pp. 1203–1211. EMAS Ltd, West Midlands (1984)

Gathercole, N., Reiter, H., Adam, T., Harris, B.: Life prediction for fatigue of T800/5245 carbon fiber composites: I. Constant amplitude loading. Int. J. Fatigue **16**, 523–532 (1994)

Ghezzo, F., Giannini, G., Cesari, F., Caligiana, G.: Numerical and experimental analysis of the interaction between two notches in carbon fibre laminates. Compos. Sci. Technol. **68**(3–4), 1057–1072 (2008)

Gope, P.C.: A method for sample size determination to estimate average fatigue life. In: Proc. of 4th ISME Conference on Mech. Engg. 1, pp. 497–501 (1994)

Gope, P.C.: Determination of sample size for estimation of fatigue life by using Weibull or log-normal distribution. Int. J. Fatigue **21**, 745–752 (1999)

Gope, P.C.: Scatter analysis of fatigue life and prediction of S–N curve. J. Fail. Anal. Prev. **12**(5), 507–517 (2012)

Graham, R.H., Raines, M., Swift, K.G., Gill, L.: Prediction of stress concentrations associated with interacting stress-raisers within aircraft design: methodology development and application. Proc. Inst. Mech. Eng., Part G, J. Aerosp. Eng. **219**, 193–203 (2005)

Hwang, W., Han, K.S.: Statistical study of strength and fatigue life of composite materials. Composites **18**(1), 47–53 (1987)

Jones, R.: Mechanics of Composite Materials (1998)

Kazemahvazi, S., Kiele, J., Zenkert, D.: Tensile strength of UD-composite laminates with multiple holes. Compos. Sci. Technol. **70**, 1280–1287 (2010)

Khashaba, U.A.: Fatigue and reliability analysis of unidirectional GFRP composites under rotating bending loads. J. Compos. Mater. **37**(4), 317–331 (2003)

Khashaba, U.A., El-Sonbaty, I.A., Selmy, A.I., Megahed, A.A.: Machinability analysis in drilling woven GFR/epoxy composites: Part I—Effect of machining parameters. Composites, Part A, Appl. Sci. Manuf. **41**, 391–400 (2010)

Liu, H., Cui, H., Wen, W., Kang, H.: Fatigue characterization of T300/924 polymer composites with voids under tension-tension and compression-compression cyclic loading. Fatigue Fract. Eng. Mater. Struct. (2017). https://doi.org/10.1111/ffe.12721

Maillet, I., Michel, L., Rico, G., Fressinet, M., Gourinat, Y.: A new test methodology based on structural resonance for mode I fatigue delamination growth in a unidirectional composite. Compos. Struct. **97**, 353–362 (2013)

Marines, I., Dominguez, G., Baudry, G., Vittori, J.F., Rathery, S., Doucet, J.P., Bathias, C.: Ultrasonic fatigue tests on bearing steel AISI-SAE 52100 at frequency of 20 and 30 kHz. Int. J. Fatigue **25**, 1037–1046 (2003)

Marwa, A.A.E., Mohamed, A.A., Madeha, K.: Flexural fatigue and failure probability analysis of polypropylene-glass hybrid fibre reinforced epoxy composite laminates. Plast. Rubber Compos. (2017). https://doi.org/10.1080/14658011.2017.1397252

Meguid, S.A., Gong, S.X.: Stress concentration around interacting circular holes: a comparison between theory and experiments. Eng. Fract. Mech. **44**(2), 247–256 (1993)

Mohamed, N.S., Ying, W., Arief, Y., Adam, J., Prasad, P., Gilles, L., Soutis, C.: Investigating the potential of using off-axis 3D woven composites in composite joints' applications. Appl. Compos. Mater. (2016). https://doi.org/10.1007/s10443-016-9529-9

Nakazawa, H., Kodama, S.: Statistical research on fatigue and fracture. In: Tanaka, T., Nishijima, S., Ichikawa, M. (eds.) Current Japanese Materials Research 2, vol. 2, pp. 59–69. Elsevier, Amsterdam (1987)

Parida, N., Das, S.K., Gope, P.C., Mohanty, O.N.: Probability, confidence and sample size in fatigue testing. J. Test. Eval. **18**(6), 385–389 (1990)

Ratnaparkhi, M.V., Park, W.J.: Lognormal distribution-model for fatigue life and residual strength of composite materials. IEEE Trans. Reliab. **35**(3) (1986)

Sakin, R., Irfan, A.: Statistical analysis of bending fatigue life data using Weibull distribution in glass-fiber reinforced polyester composites. Mater. Des. **29**, 1170–1181 (2008)

Satapathy, M.R., Vinayak, B.G., Jayaprakash, K., Naik, N.K.: Fatigue behaviour of laminated composites with a circular hole under in-plane multiaxial loading. Mater. Des. **51**, 347–356 (2013)

Shimokava, T., Hamaguchi, Y.: Distributions of fatigue life and fatigue strength in notched specimens of a carbon eight-harness-satin laminate. J. Compos. Mater. **17**(1), 64–76 (1983)

Shimokawa, T., Hamaguchi, Y.: Fatigue life distributions of notched graphite/epoxy composite specimens. J. Soc. Mat. Sci. **30**, 373–379 (1981)

Sohar, C.R., Betzwar-Kotas, A., Gierl, C., Weiss, B., Danninger, H.: Gigacycle fatigue behavior of a high chromium alloyed cold work tool steel. Int. J. Fatigue **30**(7), 1137–1149 (2008)

Soutis, C., Fleck, N.A., Smith, P.A.: A compression fatigue behaviour of notched carbon fiber epoxy laminates. Int. J. Fatigue **13**, 303–312 (1991)

Vassilopoulos, A.P.: Introduction to Fatigue Life Prediction of Composites and Composite Structures. Woodhead Publishing, New Delhi (2010)

Wei-xun, F., Jian-guo, W.: Stress concentration of a laminate weakened by multiple holes. Compos. Struct. **10**, 303–319 (1988)

Wicaksono, S., Chai, G.B.: A review of advances in fatigue and life prediction of fiber-reinforced composites. J. Mater.: Des. Appl. **227**(3), 179–195 (2012)

Xu, X.W., Man, H.C., Yue, T.M.: Strength prediction of composite laminates with multiple elliptical holes. Int. J. Solids Struct. **37**, 2887–2900 (2000)

Yang, J.N., Jones, D.L.: Statistical fatigue of graphite/epoxy angle-ply laminates in shear. J. Compos. Mater. **12**, 371–389 (1978)

Yang, J.N., Miller, R.K., Sun, C.T.: Effect of high load on statistical fatigue of unnotched graphite/epoxy laminates. J. Compos. Mater. **14**, 82–94 (1980)